Use of Ionic Liquids in the Synthesis of Nanocrystals and Nanorods of Semiconducting Metal Chalcogenides

ARTICLE *in* CHEMISTRY · OCTOBER 2007

Impact Factor: 5.73 · DOI: 10.1002/chem.200601733 · Source: PubMed

DOI: 10.1002/chem.200601733

Use of Ionic Liquids in the Synthesis of Nanocrystals and Nanorods of Semiconducting Metal Chalcogenides

Kanishka Biswas[a, b] and C. N. R. Rao*[a, b]

Abstract: We have synthesized nanoparticles of hexagonal CdS in the diameter range 3–13 nm by the reaction of cadmium acetate dihydrate with thioacetamide in imidazolium [BMIM]-based ionic liquids. We have obtained three different particle sizes of CdS by changing the anion of the ionic liquid. Addition of trioctylphosphine oxide (TOPO) to the reaction mixture causes greater monodispersity as well as smaller particle size, while addition of ethylenediamine produces nanorods of 7 nm average diameter. Hexagonal ZnS and cubic PbS nanoparticles with average diameters of 3 and 10 nm, respectively, have been prepared by the reaction of the metal acetates with thioacetamide in [BMIM][BF_4]. Hexagonal CdSe nanoparticles with an average diameter 12 nm were obtained by the reaction of cadmium acetate dihydrate with dimethylselenourea in [BMIM]-[BF_4]. In this case also we observe the same effect of the addition of TOPO as in the case of CdS. Addition of ethylenediamine to the reaction mixture gives rise to nanorods. ZnSe nanowires with a cubic structures, possible diameters in the range 70–100 nm by the reaction of zinc acetate dihydrate with dimethylselenourea in [BMIM]-[$MeSO_4$]. The nanostructures obtained are single crystalline in all the cases. Most of the nanostructures show characteristic UV/Vis absorption and photoluminescence emission spectra. The thermodynamically most stable structures are generally produced in the synthesis carried out in ionic liquids.

Keywords: ionic liquids · metal chalcogenides · nanocrystals · nanorods · nanostructures

Introduction

Nanocrystals and nanorods of inorganic materials have been prepared by a variety of methods, especially those involving solvothermal and hydrothermal techniques.[1] In the last two to three years, there have been attempts to use ionic liquids as media for the synthesis of inorganic nanomaterials.[2,3] The low interface tension and the associated high nucleation rate as well as high thermal stability make ionic liquids an attractive reaction medium for the synthesis of nanostructures. Ionic liquids have received much attention due to their potential use as green recyclable alternatives to traditional organic solvents. Ionic liquids are organic salts with low melting points and no measurable vapour pressure, and do not evaporate. They remain liquid over a wide range of temperatures, in some cases above 400 °C. The cation and anion of an ionic liquid are selected to create a degree of asymmetry. This asymmetry prevents crystallization of the salt by frustration in packing. However, there have been very few reports in the literature on the synthesis of nanostructures of important inorganic nanomaterials such as metal chalcogenides in ionic liquids. Nanoparticles of Rh and Ir have been prepared by reduction of the appropriate compounds in 1-*n*-butyl-3-methylimidazolium hexafluorophosphate, ([BMIM][PF_6]), in the presence of hydrogen.[4] Synthesis and functionalization of gold nanoparticles in ionic liquids is also reported, wherein the colour of the gold nanoparticles can be tuned by changing the anion of ionic liquid.[5] Single crystalline Te nanorods and nanowires have been prepared by microwave-assisted synthesis in a mixture of *n*-butylpyridinium tetrafluoroborate and polyvinylpyrrolidone.[6] We considered it rewarding to explore the use of ionic liquids for the synthesis semiconducting metal chalcogenides.

Nanostructures of semiconducting metal chalcogenides have been prepared generally by solvothermal methods. Gautam et al.[7] prepared organic soluble CdS nanocrystals

[a] K. Biswas, Prof. Dr. C. N. R. Rao
Chemistry and Physics of Materials Unit
DST unit on Nanoscience and
CSIR Centre of Excellence in Chemistry
Jawaharlal Nehru Centre for Advanced Scientific Research
Jakkur P.O., Bangalore 560064 (India)
Fax: (+91) 80-2208-2760
E-mail: cnrrao@jncasr.ac.in

[b] K. Biswas, Prof. Dr. C. N. R. Rao
Solid State and Structural Chemistry Unit
Indian Institute of Science, Bangalore 560012 (India)

by the solvothermal reaction of cadmium stearate with sulfur in presence of tetralin in toluene at 220 °C. CdSe nanoparticles were similarly prepared solvothermally by the reaction of cadmium stearate with selenium powder.[8] Nearly monodispersed Cd–chalcogenide nanocrystals (CdE, E = S, Se, Te) have been synthesized by the pyrolysis of organometallic reagents such as alkyl cadmium injecting in a hot coordinating solvent in the presence of silylchalcogenides/phosphinechalcogenides.[9] Nanocrystals of Cd and Zn sulfides and selenides are also obtained by the thermolysis of dithio or diselenocarbamato complexes in trioctylphosphine oxide (TOPO).[10,11] Aligned arrays of ZnSe nanowires and nanorods can be fabricated by metal-organic chemical vapour deposition.[12] Nanoparticles of PbS have been prepared by the sonochemical irradiation of a solution of elemental sulfur and lead acetate in ethylenediamine.[13] In this article, we report the results of our investigations on the synthesis nanostructures of CdS, CdSe, ZnS, ZnSe and PbS using the media of ionic liquids. We have examined the effects of changing the anion of the ionic liquid, as well as the addition of surfactants and capping agents on the size and shape of the nanostructures obtained.

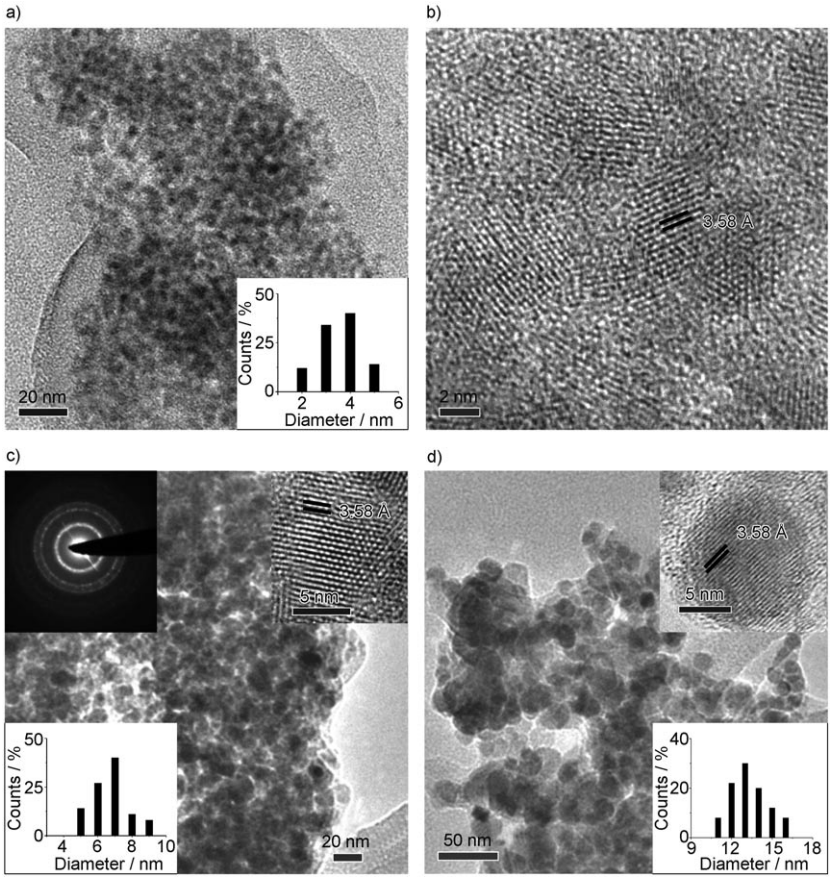

Figure 1. a) TEM image of 4 nm CdS nanoparticles prepared in [BMIM][$MeSO_4$]; the lower inset in a) shows the size distribution histogram; b) HREM image of these nanoparticles; c) and d) TEM images of 7 and 13 nm CdS nanoparticles prepared in [BMIM][BF_4] and [BMIM][PF_6], respectively. Upper insets in c) show the SAED pattern and a HREM image of the 7 nm CdS nanoparticles and the lower inset shows the size distribution histogram. Upper inset in d) shows the HREM image and the lower inset in d) shows the size distribution histogram of the 13 nm CdS nanoparticles.

Results and Discussion

Metal sulfides: In Figure 1a, we show the TEM image of the CdS nanoparticles prepared in [BMIM][$MeSO_4$]. The particles are reasonably monodisperse with an average diameter of 3 nm as can be seen from the size distribution histogram in the inset of Figure 1a. The nanocrystals were single crystalline as indicated by the HREM image of the 3 nm nanocrystals in Figure 1b. The image shows a lattice spacing of 3.58 Å corresponding to the (100) planes of hexagonal CdS nanoparticles. Figure 2a shows the XRD pattern of the CdS nanoparticles prepared in [BMIM][$MeSO_4$]. The patterns could be indexed on the hexagonal ($P6_3mc$) space group ($a = 4.136$ and $c = 6.713$ Å, JCPDS no. 77-2306). A TEM image of CdS nanoparticles obtained by the use of [BMIM][BF_4] is shown in Figure 1c. The lower inset in Figure 1c shows the size distribution histogram of the CdS nanoparti-

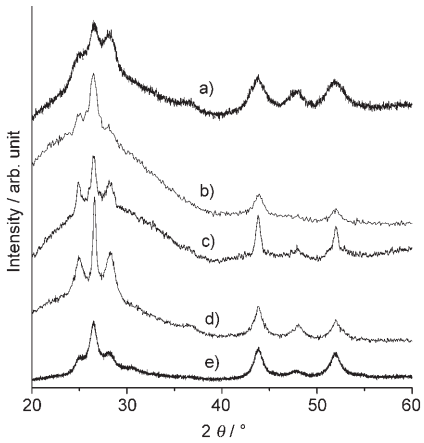

Figure 2. XRD patterns of a) 4 nm CdS nanoparticles, b) 7 nm CdS nanoparticles, c) 13 nm CdS nanoparticles, d) CdS nanorods and e) TOPO-capped 4 nm CdS nanoparticles.

cles, indicating the average diameter to be 7 nm. The upper insets in Figure 1c show the selected area electron diffraction (SAED) pattern CdS nanoparticles and the HREM image of a single 7 nm nanoparticle. The lattice spacing of 3.58 Å corresponding to the (100) planes of hexagonal CdS nanoparticles is clearly seen in the HREM image. The XRD pattern of these hexagonal CdS nanoparticles is shown in Figure 2b ($P6_3mc$ space group, $a=4.136$ and $c=6.713$ Å, JCPDS no. 77-2306). A TEM image of the CdS nanoparticles prepared in [BMIM][PF_6] is shown in Figure 1d, with the size distribution histogram as the lower inset. The average diameter of the nanoparticles is 13 nm. A HREM image of a single nanocrystal given in the top inset of Figure 1d shows a lattice spacing of 3.58 Å. In Figure 2c, we show the XRD pattern of these nanoparticles. The pattern also indexed based on the hexagonal ($P6_3mc$) space group ($a=$ 4.136 and $c=6.713$ Å, JCPDS no. 77-2306). We thus found out that the particle size of the CdS nanoparticles varies between 3 and 13 nm with the anion of imidazolium-based ionic liquid under the same reaction conditions. A similar observation has been reported in the case of gold nanoparticles.[5]

In Figure 3A, we show the UV/Vis absorption spectra of CdS nanoparticles with average diameters of 3, 7 and 13 nm prepared in [BMIM][$MeSO_4$], [BMIM][BF_4] and [BMIM]-[PF_6] respectively. We observed a band in the 460 nm region.[7,11] The UV/Vis absorption band shifts towards higher wavelength with increasing particle size of the nanoparticles. Figure 3B depicts the photoluminescence spectra of the CdS nanoparticles, exhibiting a band in the 500 nm region.[10,11] The PL bands of three different nanoparticles are red-shifted (Stokes shifted) in the relation to the corresponding absorption spectra, suggesting the band-edge (or near band-edge) luminescence characteristics of these materials.[10,11] The PL band maximum values are 487, 515 and 540 nm, respectively, for nanocrystals with average diameters of 3, 7, and 13 nm, showing that the PL band shifts to higher wavelengths with increasing particle size.

The synthesis of CdS nanoparticles carried out in [BMIM][BF_4] in the presence of TOPO gives nearly monodisperse CdS particles as shown by the TEM image in Figure 4a. From the size distribution shown as the upper inset of this Figure we see the average diameter to be 4 nm. The use of TOPO results greater monodispersity as well as smaller size of the particle. The lower inset in Figure 4a shows a HREM image of a single 4 nm CdS nanoparticle. The lattice spacing of 3.58 Å corresponding to the (100) planes of hexagonal CdS nanoparticles is clearly seen in the HREM image. The XRD pattern of these particles shown in Figure 2e. The pattern could be indexed on the hexagonal ($P6_3mc$) space group ($a=4.136$ and $c=6.713$ Å, JCPDS no. 77-2306). Inset in Figure 3a shows the UV/Vis absorption spectrum (open circles) of TOPO-capped CdS nanoparticles of average diameter 4 nm. The absorption band of TOPO-capped nanoparticles is at 460 nm, getting 15 nm blue shifted compared with the uncapped 7 nm CdS nanoparticles prepared in only [BMIM][BF_4]. The PL spectrum (open circles) of these nanoparticles is shown as inset in Figure 3b. PL band maximum of the TOPO-capped 4 nm CdS nanoparticles is at 503 nm, getting 12 nm blue shifted compared with the uncapped 7 nm CdS nanoparticles prepared in only [BMIM][BF_4].

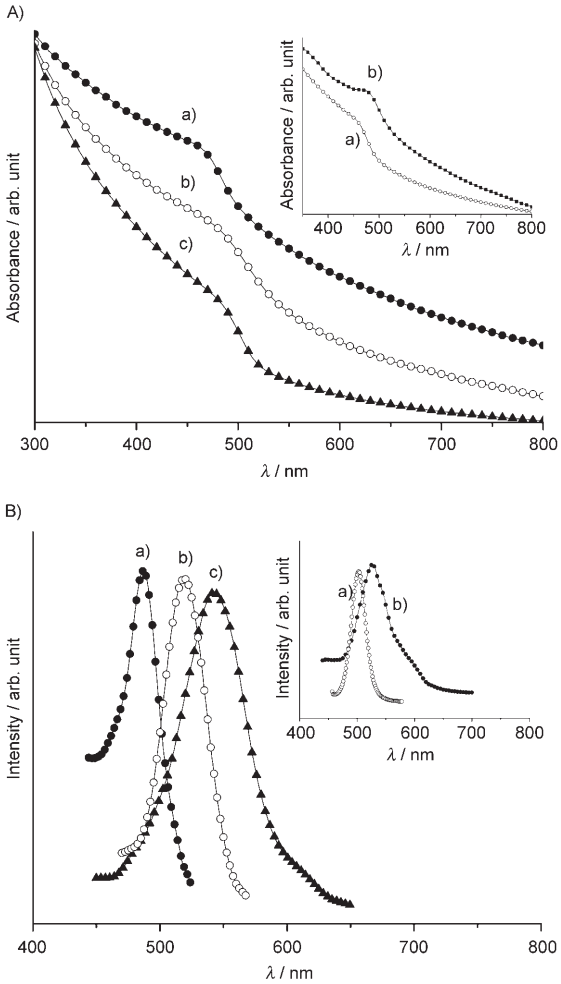

Figure 3. A) UV/Vis absorption spectra of CdS nanoparticles of diameters a) 4 nm, b) 7 nm and c) 13 nm. Inset in A) shows the UV/Vis absorption spectra of a) TOPO-capped CdS nanoparticles (○) and b) CdS nanorods prepared using ethylenediamine (●). B) PL spectra of CdS nanoparticles of average diameters a) 4 nm, b) 7 nm and c) 13 nm. Inset in B) shows the PL spectra of a) TOPO-capped CdS nanoparticles (○) and b) CdS nanorods prepared using ethylenediamine (●).

The reaction carried out in [BMIM][BF_4] in the presence of ethylenediamine gives nanorods for CdS. Figure 4b shows a TEM image of the CdS nanorods. From the diameter distribution shown in the bottom inset of this figure, we found the average diameter to be around 7 nm. The upper inset in Figure 4b shows a HREM image of a single 7 nm diameter CdS nanorod. The image shows a lattice spacing of 3.58 Å corresponding to the (100) planes of hexagonal CdS nanorod. The XRD pattern of the nanorods is shown in Figure 2d. The pattern could be indexed on the hexagonal ($P6_3mc$) space group ($a=4.136$ and $c=6.713$ Å, JCPDS no. 77-2306). The inset in Figure 3a shows the UV/Vis absorp-

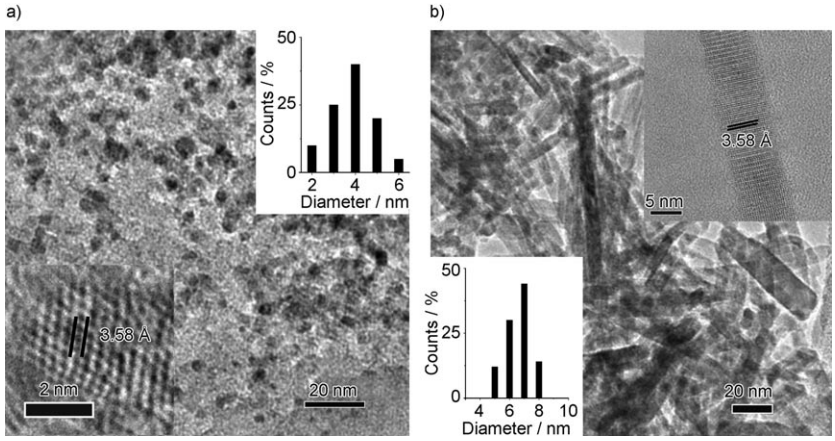

Figure 4. a) TEM image of TOPO-capped CdS nanoparticles. Upper inset in a) shows the size distribution histogram and the lower inset shows the HREM image of the 4 nm TOPO-capped CdS nanoparticle. b) TEM image of CdS nanorods prepared in a [BMIM][BF_4] and ethylenediamine mixture. Lower inset in b) shows the size distribution histogram and the upper inset shows a HREM image of a nanorod.

tion spectrum (filled circles) of CdS nanorods of average diameter 7 nm. It shows an absorption band around 480 nm. The PL spectrum (filled circles) of the 7 nm diameter CdS nanorods is shown as an inset in Figure 3b. PL band maximum of CdS nanorods is at 525 nm.

Figure 5a and b shows the TEM images with size distribution histograms of ZnS and PbS nanoparticles prepared in [BMIM][BF_4]. The average diameters are 3 and 10 nm for the ZnS and PbS nanoparticles, respectively. The particles are reasonably monodisperse in both the cases. The lower inset in Figure 5a shows a single particle HREM image of a 3 nm ZnS nanoparticle. The image shows a lattice spacing of 3.30 Å corresponding to the (100) planes of hexagonal ZnS. The upper inset in Figure 5b shows a single particle HREM image of a 10 nm PbS nanoparticles with a lattice spacing 3.4 Å corresponding to the (111) planes of cubic PbS. In Figure 6, we show the XRD patterns of the ZnS and PbS nanoparticles. The (100), (002) and (101) reflections of hexagonal ZnS merge to form a broad band in the XRD pattern in Figure 6a due to small particle size. The XRD pattern could be indexed on the hexagonal ($P6_3mc$) space group ($a=3.820$ and $c=6.257$ Å, JCPDS no. 36-1450). The XRD pattern of PbS nanoparticles in Figure 6b could be indexed on the cubic ($Fm3m$) space group ($a=$ 5.931 Å, JCPDS no. 78-1901). We measured the optical properties of the ZnS nanoparticles. The UV/Vis absorption spectrum of ZnS nanoparticles shows characteristic absorption band around 320 nm[11] and while the PL spectrum shows a band at 420 nm.[11,14,15] The 420 nm band is attributed to sulfur vacancies in ZnS lattice.[14,15]

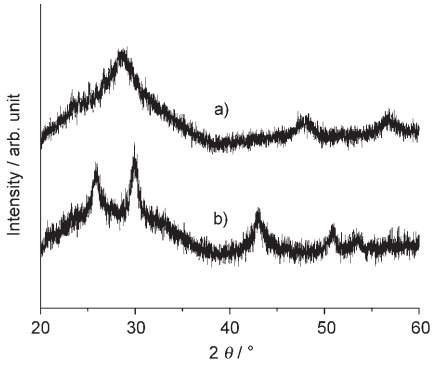

Figure 6. XRD patterns of a) 3 nm ZnS and b) 10 nm PbS nanoparticles.

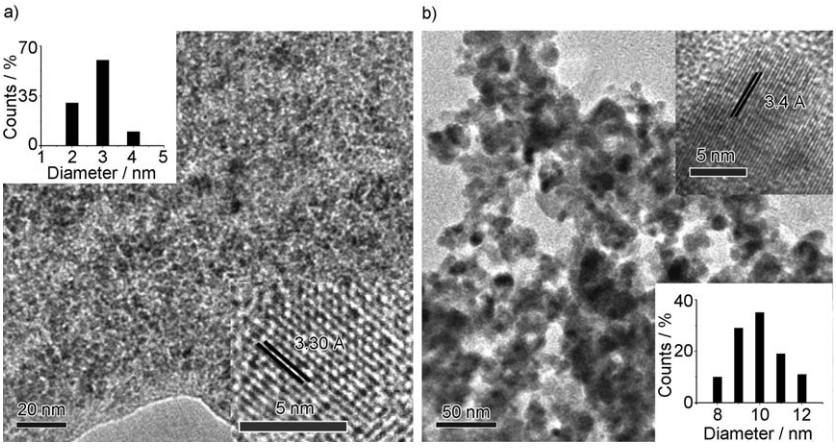

Figure 5. a) and b) TEM images of 3 nm ZnS and 10 nm PbS nanoparticles prepared in [BMIM][BF_4]. Upper inset in a) shows the size distribution histogram of ZnS nanoparticles and the lower inset shows a HREM image. Upper inset in b) shows a HREM image of a PbS nanoparticle and the lower inset shows the size distribution histogram.

Metal selenides: In Figure 7a, we show the TEM image of CdSe nanoparticles prepared in [BMIM][BF_4]. The upper and lower insets in Figure 7a show the size distribution histogram and a HREM image. The average particle size is around 12 nm. The lattice spacing of 3.50 Å in the HREM image corresponds to the (100) planes of hexagonal CdSe nanoparticles. In Figure 8a, we show the XRD pattern of these CdSe nanoparticles. The XRD pattern could be indexed on the

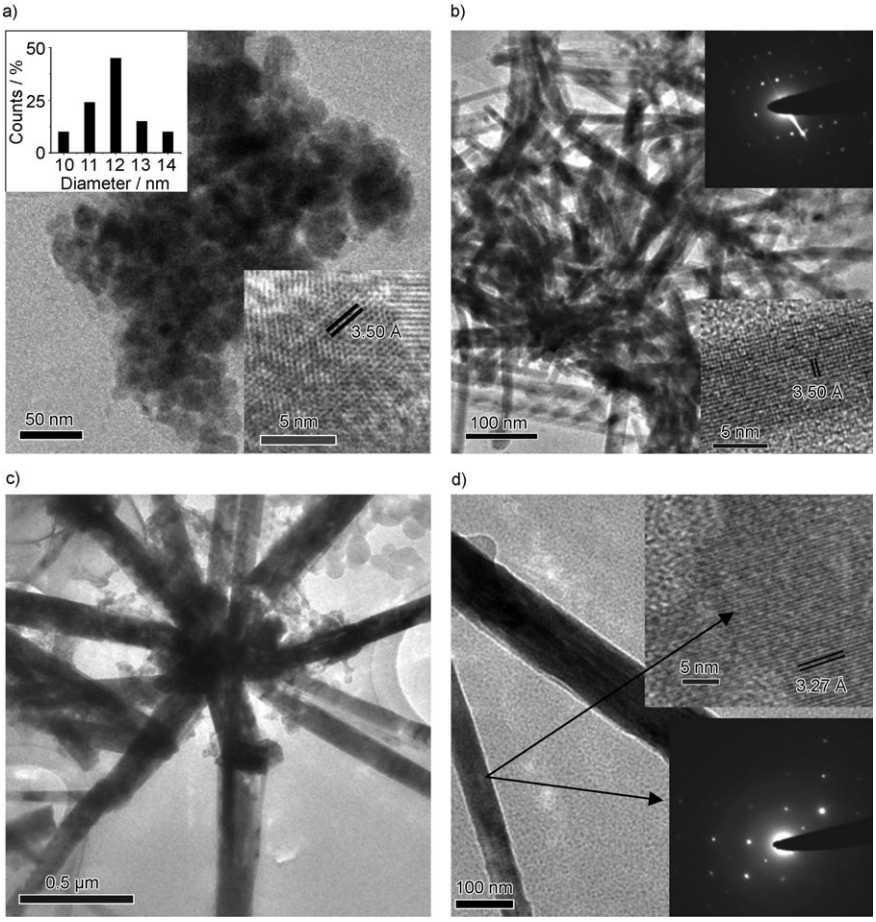

Figure 7. a) TEM image of CdSe nanoparticles prepared in [BMIM][BF_4]. Upper inset shows the size distribution histogram and the lower inset shows a HREM image of a nanoparticle. b) TEM image of CdSe nanorods. Upper inset shows the electron diffraction (ED) pattern and the lower inset shows a HREM image of a nanorod. c) and d) TEM images of ZnSe nanorods prepared in [BMIM][$MeSO_4$]. Upper inset in d) shows a HREM image of a single nanorods and the lower inset in d) shows the ED pattern from a single nanorod.

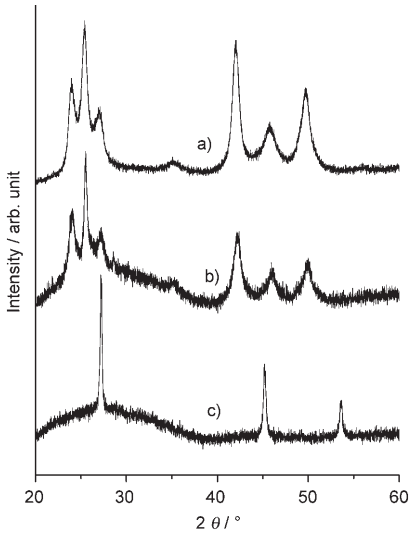

Figure 8. XRD patterns of a) 12 nm CdSe nanoparticles, b) CdSe nanorods and c) ZnSe rods.

hexagonal ($P6_3mc$) space group ($a=4.299$ and $c=7.010$ Å, JCPDS no. 77-2307). The synthesis of CdSe nanoparticles carried out in [BMIM][BF_4] in the presence of TOPO gives nearly monodisperse CdSe particles of average diameter of 9.5 nm. The XRD pattern of the nanoparticles could be indexed on the hexagonal ($P6_3mc$) space group ($a=4.299$ and $c=7.010$ Å, JCPDS no. 77-2307). TEM image of these nanoparticles shows quite good monodispersity in particle size. The particles are single crystalline as indicated by HREM image. The particles shows UV/Vis absorption band around 540 nm and PL emission band around 620 nm.[9,11] Figure 7b shows a TEM image of CdSe nanorods with an average diameter 10 nm obtained in the presence of ethylenediamine. The upper inset in Figure 7b shows the SAED pattern from a single nanorod. The lower inset in Figure 7b shows a HREM image of a single nanorod with a lattice spacing of 3.50 Å corresponds to the (100) planes. In Figure 8b, we show the XRD patterns of the CdSe nanorods. The XRD pattern could be indexed on the hexagonal ($P6_3mc$) space group ($a=4.299$ and $c=7.010$ Å, JCPDS no. 77-2307).

Figure 7c and d shows the TEM images of ZnSe nanorods obtained in [BMIM][$MeSO_4$] without using any amine. The upper inset in Figure 7d shows a HREM image of a single ZnSe nanorod with a lattice spacing of 3.27 Å corresponding to the (100) planes. In the lower inset of Figure 7d, we show the SAED pattern of a single ZnSe nanorod. The XRD pattern of the nanorods in Figure 8c could be indexed on the cubic ($F\bar{4}3m$) space group ($a=5.668$ Å, JCPDS no. 37–1463). The UV/Vis spectrum of the ZnSe nanorods shows a band around 280 nm.[16]

The success of ionic liquids in the synthesis of inorganic nanostructures, and of the semiconducting metal chalcogenides in particular, can be understood based on the following considerations. Owing to the high thermal stability of ionic liquids, we could perform the reactions well above 150 °C, but we carried out the reaction at 180 °C which is below the temperature normally employed for solvothermal reaction.[7,8] The synthesis could also be performed under

anhydrous conditions. In the synthesis of metal chalcogenide nanostructures, the ionic liquids also play a dual role, acting as solvents as well as stabilizers. In the ionic liquid medium, the decomposition of the metal acetate gives rise to solvated metal cations, along with the gaseous oxides of carbon. Reaction of the metal cations with the chalcogenide anions gives rise to metal chalcogenide. As soon as the metal chalcogenide nanocrystal nuclei are formed, they get coated by the ionic liquid, thereby producing a control on the growth. The low interfacial tension of ionic liquids gives rise to high nucleation rates, thus enabling the generation of small nanoparticles which undergo Ostwald ripening only weakly. The combined intrinsic high charge plus the steric bulk of these salts is considered to be responsible for creating an electrostatic and steric (colloid-type) stabilization of metal chalcogenide nanoparticles. Ionic liquids form extended hydrogen-bond systems in liquid state[2] and are therefore highly structured. This special feature acts as an entropic driver for spontaneous, well-defined and extended ordering of nanoscale metal chalcogenides.

We have obtained different sizes of CdS nanoparticles by changing the anion of the ionic liquid. The stabilization effect of the ionic liquid appeared to change with the anion of imidazolium-based ionic liquids, thereby giving rise to particles of different sizes. The formation of metal chalcogenide nanorods in a mixture of ethylenediamine and an ionic liquid indicates the effect of the amine which acts as a structure-directing agent. Amines are known to favour the formation of one-dimensional nanostructures.

Conclusion

We have been able to prepare single crystalline nearly monodisperse nanostructures of the semiconducting metal chalcogenides, CdS, ZnS, PbS, CdSe and ZnSe, by carrying out the reaction of metal salts with the sulfiding or seleniding agent in ionic liquids around 180 °C. The reactions proceed smoothly in the medium of ionic liquids, readily giving rise to the metal chalcogenide nanocrystals and nanorods. Metal chalcogenides are generally synthesized by solvothermal methods using high boiling solvents and capping agents in the 220–300 °C range. Interestingly, the anion plays a role in determining the size of the nanocrystals. We obtained nanorods of the metal chalcogenides by adding ethylenediamine to the reaction mixture. In the case of ZnSe, we obtain nanorods even without the addition of ethylenediamine. In the ionic liquid medium, we appear to generally obtain thermodynamically stable phases of the metal chalcogenide nanostructures.

Experimental Section

The methods employed by us to prepare the nanostructures of semiconducting metal chalcogenides were based on the decomposition of metal acetates at relatively low temperatures in the presence of sulfur/selenium producing reagents in the media of imidazolium-based ionic liquids. In the first set of experiments, decomposition of cadmium acetate dihydrate (25 mg, 0.09 mmol) was carried out in the presence of thioacetamide (7.3 mg, 0.09 mmol) in 1-butyl-3-methylimidazolium methylsulfate, ([BMIM][$MeSO_4$]) (1 mL), in a 7 mL Teflon-lined stainless still autoclave at 180 °C for 5 h. We repeated this experiment with 1-butyl-3-methylimidazolium tetrafluoroborate, ([BMIM][BF_4]), and 1-butyl-3-methylimidazolium hexafluorophosphate, ([BMIM][PF_6]), keeping the other conditions the same. In order to study the effect of a capping agent, cadmium acetate dihydrate (25 mg, 0.09 mmol) was decomposed in the presence of thioacetamide (7.3 mg, 0.09 mmol) and TOPO (17. 9 mg, 0.046 mmol) in [BMIM][BF_4] (1 mL). In another preparation, cadmium acetate dihydrate (25 mg, 0.09 mmol) was decomposed in the presence of thioacetamide (7.3 mg, 0.09 mmol) in a mixture of [BMIM][BF_4] (1 mL) and ethylenediamine (1 mL). ZnS nanostructures were prepared by the decomposition of zinc acetate dihydrate (25 mg, 0.11 mmol) in the presence of thioacetamide (8.5 mg, 0.11 mmol) in [BMIM][BF_4] (1 mL), in a 7 mL Teflon-lined stainless still autoclave at 180 °C for 5 h. PbS nanostructures were prepared by the decomposition of lead acetate trihydrate (25 mg, 0.065 mmol) in the presence of thioacetamide (5 mg, 0.065 mmol) in [BMIM][BF_4] (1 mL), in a 10 mL round bottom flask at 100 °C for 15 min.

We prepared the nanostructures of the metal selenides as follows. CdSe nanoparticles were prepared by the decomposition of cadmium acetate dihydrate (25 mg, 0.093 mmol) in the presence of dimethylselenourea (14 mg, 0.093 mmol) in [BMIM][BF_4] (1 mL), in a 7 mL Teflon-lined stainless still autoclave at 180 °C for 5 h. In order to study the effect of a capping agent, cadmium acetate dihydrate (25 mg, 0.09 mmol) was decomposed in the presence of dimethylselenourea (14 mg, 0.093 mmol) and TOPO (17. 9 mg, 0.046 mmol) in [BMIM][BF_4] (1 mL). CdSe nanorods also obtained by using ethylenediamine (1 mL) keeping the other reaction parameters the same as for the CdSe nanoparticle synthesis. ZnSe nanostructures were prepared by the decomposition of zinc acetate dihydrate (15 mg, 0.07 mmol) in the presence of dimethylselenourea (10.3 mg, 0.0.07 mmol) in [BMIM][$MeSO_4$] (1 mL), in a 7 mL Teflon-lined stainless still autoclave at 180 °C for 2 h. We did not use ethylenediamine as the capping agent here. For reasons that are not clear, we did not obtain good ZnSe structures when [BMIM][BF_4] was used as medium. In all the cases, the as-prepared nanostructures were thoroughly washed with double distilled water and ethanol for several times.

The nanostructures were characterized by powder X-ray diffraction (XRD) using a Phillips X′Pert diffractometer employing the Bragg–Brentano configuration. The XRD patterns of the nanocrystals show a broad background maximum in the 2θ range of 20–30° probably due to the small coverage of the metal chalcogenide nanoparticles by the ionic liquids. A Similar background has been observed in the case of TOPO-capped CdS[7] and CdSe[17] nanoparticles. Thermo gravimetric analysis (TGA) analysis shows that the small coverage of the ionic liquid is removed below 500 °C. TEM images of the nanostructures were obtained by taking a drop of ethanol solution on the holey carbon-coated Cu grids. The grids were allowed to dry in the air and examined by using a JEOL (JEM3010) microscope operating with an accelerating voltage of 300 kV. Photoluminescence (PL) measurements were made with a Perkin-Elmer LS 50B luminescence spectrophotometer fitted with a Xenon lamp excitation source (200–900 nm). UV/Vis absorption spectra were recorded using a Perkin-Elmer Lambda 900 UV/VIS/NIR spectrophotometer (200–3300 nm).

[1] a) *The Chemistry of Nanomaterials* (Eds.: C. N. R. Rao, A. Mueller, A. K. Cheetham), Wiley-VCH, Weinheim, **2004**; b) G. Schmid, *Nanoparticles: Theory to Application*, Wiley-VCH, Weinheim, **2004**; c) C. Burda, X. Chen, R. Narayanan, M. A. El-Sayed . *Chem. Rev.* **2005**, *105*, 1025–1102; d) C. N. R. Rao, A. Govidaraj, *Nanotubes and Nanowires*, RSC, **2006**.
[2] M. Antonietti, D. Kuang, B. Smarsly, Y. Zhou, *Angew. Chem.* **2004**, *116*, 5096–5100; *Angew. Chem. Int. Ed.* **2004**, *43*, 4988–4992.
[3] Y. Zhou, *Curr. Nanoscience* **2005**, *1*, 35–42.

[4] G. S. Fonseca, A. P. Umpierre, P. F. P. Fichtner, S. R. Teixeira, J. Dupont, *Chem. Eur. J.* **2003**, *9*, 3263–3269.
[5] H. Itoh, K. Naka, Y. Chujo, *J. Am. Chem. Soc.* **2004**, *126*, 3026–3027.
[6] Y.-J. Zhu, W.-W. Wang, R.-J. Qi, X.-L. Hu, *Angew. Chem.* **2004**, *116*, 1434–1438; *Angew. Chem. Int. Ed.* **2004**, *43*, 1410–1414.
[7] U. K. Gautam, R. Seshadri, C. N. R. Rao, *Chem. Phys. Lett.* **2003**, *375*, 560–564.
[8] U. K. Gautam, M. Rajamathi, F. Meldrum, P. Morgan, R. Seshadri, *Chem. Commun.* **2001**, 629–630.
[9] C. B. Murray, D. J. Norris, M. G. Bawendi, *J. Am. Chem. Soc.* **1993**, *115*, 8706–8715.
[10] T. Trindade, P. O'Brien, X. Zhang, *Chem. Mater.* **1997**, *9*, 523–530.
[11] M. A. Malik, N. Revaprasadu, P. O'Brien, *Chem. Mater.* **2001**, *13*, 913–920.
[12] X. Zhang, Z. Liu, Q. Li, Y. Leung, K. Ip, S. Hark, *Adv. Mater.* **2005**, *17*, 1405–1410.
[13] J. Zhu, S. Liu, O. Palchik, Y. Koltypin, A. Gedanken, *J. Solid State Chem.* **2000**, *153*, 342–348.
[14] P. Hu, Y. Liu, L. Fu, L. Cao, D. Zhu, *J. Phys. Chem. B* **2004**, *108*, 936–938.
[15] S. Wageh, Z. S. Ling, X. X. Rong, *J. Cryst. Growth* **2003**, *255*, 332–337.
[16] F. T. Quilan, J. Kuther, W. Tremel, W. Knoll, S. Risbud, P. Strove, *Langmuir* **2000**, *16*, 4049–4051.
[17] D. J. Crouch, P. O'Brien, M. A. Malik, P. J. Skabara, S. P. Wright, *Chem. Commun.* **2003**, 1454–1455.

Received: December 4, 2006
Revised: February 21, 2007
Published online: May 11, 2007

